Received: 24 June 2023 | Accepted: 6 October 2023

DOI: 10.1002/prp2.1149

ORIGINAL ARTICLE

The roles of CYP2C19 and CYP3A4 in the in vitro metabolism of β-eudesmol in human liver: Reaction phenotyping and enzyme kinetics

Nadda Muhamad[1,2] | Kesara Na-Bangchang[1,2,3]

[1]Graduate Studies, Chulabhorn International College of Medicine, Thammasat University, Pathumthani, Thailand

[2]Center of Excellence in Pharmacology and Molecular Biology of Malaria and Cholangiocarcinoma, Thammasat University, Pathumthani, Thailand

[3]Drug Discovery and Development Center, Office of Advanced Science and Technology, Thammasat University, Pathumthani, Thailand

Correspondence
Kesara Na-Bangchang, Graduate Studies, Chulabhorn International College of Medicine, Thammasat University, Pathumthani 12120, Thailand.
Email: kesaratmu@yahoo.com

Funding information
Center of Excellence in Pharmacology and Molecular Biology of Malaria and Cholangiocarcinoma; Thailand Science Research and Innovation Fundamental Fund; Thammasat University Research Fund, Grant/Award Number: TUFT-FF 48/2565; The Thailand Research Fund under the Royal Golden Jubilee Ph.D. Program, Grant/Award Number: PHD/0095/2561

Abstract

β-eudesmol is a major bioactive component of *Atractylodes lancea* (AL). AL has been developed as the capsule formulation of standardized AL extract for treating cholangiocarcinoma (CCA). However, the complex constituents of herbal products increase the risk of adverse drug interactions. β-eudesmol has demonstrated inhibitory effects on rCYP2C19 and rCYP3A4 in the previous research. This study aimed to identify the cytochrome P450 (CYP) isoforms responsible for the metabolism of β-eudesmol and determine the enzyme kinetic parameters and the metabolic stability of β-eudesmol metabolism in the microsomal system. Reaction phenotyping using human recombinant CYPs (rCYPs) and selective chemical inhibitors of CYP1A2, CYP2C9, CYP2C19, CYP2D6, and CYP3A4 was performed, and enzyme kinetics and metabolic stability were investigated using human liver microsome (HLM). The results suggest that CYP2C19 and CYP3A4 play significant roles in β-eudesmol metabolism. The disappearance half-life ($t_{1/2}$) and intrinsic clearance (CL_{int}) of β-eudesmol were 17.09 min and 0.20 mL/min·mg protein, respectively. Enzyme kinetic analysis revealed the Michaelis–Menten constant (K_m) and maximum velocity (V_{max}) of 16.76 μM and 3.35 nmol/min·mg protein, respectively. As a component of AL, β-eudesmol, as a substrate and inhibitor of CYP2C19 and CYP3A4, has a high potential for drug–drug interactions when AL is co-administered with other herbs or conventional medicines.

KEYWORDS
Atractylodes lancea (Thunb.) DC, cytochrome P450, drug metabolism, enzyme kinetics, reaction phenotyping, β-eudesmol

Abbreviation: AL, *Atractylodes lancea*; CCA, Cholangiocarcinoma; CL_{int}, Intrinsic clearance; CYP, Cytochrome P450; HLM, Human liver microsome; HPLC, High-performance liquid chromatography; IC_{50}, Concentration that inhibits enzyme activity by 50%; K_m, Michaelis–Menten constant; NADPH, Nicotinamide adenine dinucleotide phosphate tetrasodium salt-reduced form; $T_{1/2}$, Half-life; V_{max} Maximum velocity

Recommended section assignment: Metabolism, Transport, and Pharmacogenomics.

1 | INTRODUCTION

Atractylodes lancea (*A. lancea*: AL) has a long history of traditional use as medicine in various Asian countries, such as China, Japan, Korea, and Thailand.[1] The ethanolic extract of AL has shown promising anti-cholangiocarcinoma (CCA) activities in a series of our previous in vitro and in vivo studies.[2–5] Atractylodin, β-eudesmol, and hinesol are the prominent active components of AL, accounting for 14%, 6%, and 1%, respectively. These compounds have also exhibited anti-CCA activities in various investigations.[2,6,7] Notably, the combined use of these compounds produced synergistic effects on cytotoxic activity against CCA cells.[6] This led to the development of capsule formulation of the standardized AL extract for clinical use in CCA patients.[8] The phase I clinical trial in healthy Thai subjects to assess the pharmacokinetics and tolerability of AL demonstrated a satisfactory safety profile.[9] In addition, the phase IIa clinical trial in patients with advanced-stage CCA for efficacy and safety is under investigation.

Herbal medicines are widely used and are considered safe due to the long history of their traditional uses. However, the chemical complexity of herbal medicines raises concerns about potential interactions with other traditional products or prescribed medications. The cytochrome P450s (CYPs) are important oxidative enzymes responsible for the bioconversion of endogenous and exogenous compounds and contributing to metabolic drug–drug and herb-drug interactions.[10] The biotransformation of conventional drugs predominantly involves the CYP3A4 isoform, which accounts for 50% of the contribution of all CYPs, followed by CYP2D6 (30%), CYP2C9/2C19 (11%), and CYP1A2 (4%).[11,12]

AL has gained considerable attention for its impact on CYP activity. A study has demonstrated a potent inhibitory effect of an ethanolic AL extract on human CYP1A2, with an IC_{50} value of 0.36 ± 0.02 (mean ± SD) μg/mL.[13] In contrast, the inhibitory effects of the extract on CYP2C19, CYP2D6, and CYP3A4 were observed to be of a moderate nature, with respective IC_{50} values of 16.48 ± 1.04, 313.51 ± 51.90, and 54.36 ± 5.64 μg/mL.[13] Furthermore, in vivo studies conducted in rats revealed that administering AL at the maximum dose of 5000 mg/kg body weight for 1 year resulted in the induction of CYP1A2 and inhibition of CYP3A1 in liver tissues.[14] Similarly, in mice, the active constituents of AL, atractylodin and β-eudesmol, were found to inhibit CYP1A2 and CYP3A11 following prolonged daily administrations of 100 mg/kg body weight for 14 days.[15] However, β-eudesmol has demonstrated inhibitory effects on rCYP2C19 and rCYP3A4 in vitro.[15]

The information regarding the modulatory effects of candidate drugs on metabolizing enzymes holds significant importance in drug discovery and development, as it helps prevent undesired adverse effects arising from metabolic drug interactions. Nonetheless, reaction phenotyping assumes a crucial role in identifying the specific enzymes responsible for the metabolism of drugs or compounds. It not only greatly contributes to the early assessment of inter-individual pharmacokinetics for candidate drugs metabolized by polymorphic CYP isoforms,[16] such as CYP2D6,[17] CYP2C9,[18] and CYP2C19,[19] but also plays a vital role in preventing drug interactions. Notably, several anticancer agents used in CCA treatment are substrates of CYPs. These include docetaxel (CYP3A4),[20] irinotecan (CYP2B6 and CYP3A4),[21,22] paclitaxel (CYP2C8, CYP2C9, and CYP3A4),[21,23] and erlotinib (CYP3A4).[21,24] Conversely, certain anticancer drugs may exert inhibitory effects on CYPs, such as capecitabine (CYP2C9), 5-fluorouracil (CYP2C9), and sorafenib (CYP2B6, CYP2C8, and CYP2C9).[21] Currently, there is no study available on the metabolism of the active components of AL. This emphasizes the need for comprehensive reaction phenotyping of the specific compound to better understand its interactions with CYP isoforms and optimize its safe and effective use in therapeutic applications.

Thus, the present study aimed to identify CYP isoforms responsible for the metabolism of β-eudesmol, using human recombinant CYP (rCYP) and their selective inhibitors. In addition, the kinetics of the CYP enzyme and metabolic stability of β-eudesmol in the microsomal system were investigated. β-eudesmol was selected as a representative of AL bioactive constituent due to its high quantity and stability at body temperature (Table S1).

2 | MATERIALS AND METHODS

2.1 | Chemicals and enzymes

Human liver microsome (HLM), human recombinant CYPs co-expressed with P450 oxidoreductase (OR) and with or without cytochrome b_5 (Supersomes™: CYP1A2-OR, CYP2C9-OR-b_5 (Arg_{144}), CYP2C19-OR-b_5, CYP2D6-OR (Val_{374}), and CYP3A4-OR-b_5) were obtained from Corning Life Sciences. β-eudesmol was purchased from WAKO. Nicotinamide adenine dinucleotide phosphate tetrasodium salt-reduced form (NADPH), quinidine, and ketoconazole were obtained from Tokyo Chemical Industry Co., Ltd. Acetonitrile (HPLC grade) was purchased from Fisher Scientific. α-naphthoflavone was obtained from Sigma-Aldrich. Sulfaphenazole and troglitazone were purchased from Cayman Chemical Company. 1,8-Dihydroxyantraquinone (internal standard) was purchased from MERCK KGaA.

2.2 | HPLC method for β-eudesmol quantification

Quantification of β-eudesmol in the reaction mixture utilized HPLC with an Agilent Technologies 1260 Quaternary pump VL, 1260 ALS autosampler, 1260 DAD VL detector, and OpenLAB CDS Software (version C.01.04). Separation was achieved using a C-18 reversed-phase column (Thermo Hypersil Gold, 210 × 4.6 mm, 5 μm) with an isocratic mobile phase consisting of water and acetonitrile (15%:85% v/v) running at a flow rate of 1.0 mL/min, with UV detection at 200 nm. The method validation for β-eudesmol quantification included an assessment of precision and accuracy according to ICH guidline.[25] The linear range for quantitation of β-eudesmol was

established from 5 to 200 μM. The acceptance criteria mandated precision and accuracy within 15% for concentrations above the limit of quantification (LOQ) and within 20% for measurements at the LOQ concentration.

2.3 | Optimization of β-eudesmol and microsomal protein concentrations and incubation time

To ensure reaction linearity, the optimal concentrations of microsomal protein and β-eudesmol, as well as the reaction incubation time, were determined. The reaction mixture consisted of HLM in 100 mM potassium phosphate buffer (KPB, pH 7.4), β-eudesmol and NADPH in a total volume of 200 μL. Prior to the reaction, β-eudesmol (10–30 μM) was pre-incubated with HLM (0.2–0.5 mg/mL) in 100 mM KPB at 37°C for 5 min. Subsequently, 1 mM NADPH was added to initiate the reaction, which was further incubated for 10–40 min. The reaction was terminated at specified time point by adding ice-cold acetonitrile containing internal standard (200 μL), and the supernatant was separated through centrifugation at 13000×*g* (4°C) for 10 min. The β-eudesmol concentration was then analyzed with an aliquot of 20 μL of supernatant subjected to a column. The corresponding control was prepared without NADPH. The remaining amount of β-eudesmol (%) was calculated using the following equation:

$$\beta - \text{Eudesmol remaining}\,(\%) = \frac{\text{Amount of } \beta - \text{eudesmol in the test}}{\text{Amount of } \beta - \text{eudesmol in the control}} \times 100 \quad (1)$$

2.4 | Metabolic stability and intrinsic clearance of β-eudesmol

Following the optimization of linear conditions, HLM and β-eudesmol at 0.2 mg/mL and 10 μM, respectively, were selected to investigate metabolic stability and intrinsic clearance. The reaction was initiated by pre-incubating β-eudesmol with HLM in 100 mM KPB (pH 7.4) at 37°C for 5 min, followed by the addition of 1 mM NADPH, and allowed to incubate for a duration of 0–30 min. At a predetermined time point, the reaction was terminated by adding ice-cold acetonitrile containing internal standard (200 μL). Thereafter, the concentration of β-eudesmol was determined as the described method, and a corresponding control was prepared simultaneously without the addition of NADPH. The remaining amount of β-eudesmol (%) was calculated, and the substrate turnover rate (−*k*) was estimated by plotting the natural log (Ln) of the remaining amount of β-eudesmol versus time. The half-life ($t_{1/2}$) and intrinsic clearance (CL_{int}) were calculated using specific equations as follows:

$$t_{1/2} = \frac{\ln 2}{-k} \quad (2)$$

$$CL_{int} = \frac{\ln 2}{\text{In vitro } t_{1/2}} \times \frac{\text{mL incubation}}{\text{mg microsome}} \quad (3)$$

2.5 | Assay with recombinant human CYP isoforms

To identify the CYP isoform(s) involved in β-eudesmol metabolism, five isoforms of rCYPs were used: rCYP1A2, rCYP2C9, rCYP2C19, rCYP2D6, and rCYP3A4. A reaction mixture was prepared by combining β-eudesmol (10 μM) and rCYPs (20 pmol/mL) in 100 mM KPB (pH 7.4) with a total volume of 200 μL. After a pre-incubation period of 5 min, the NADPH (1 mM) was added, and the reaction mixture was incubated for 15 min. At a specified time point, the reaction was terminated and the sample was prepared for analysis. β-eudesmol concentration was determined as previously described. The corresponding control was prepared simultaneously without the addition of NADPH. The remaining amount of β-eudesmol was calculated.

2.6 | Assays with chemical inhibitors of CYPs

To confirm the specific CYP isoform(s) responsible for the metabolism of β-eudesmol, selective chemical inhibitors of each CYP isozyme were employed in the microsomal system. The selective inhibitors used for CYP1A2, CYP2C9, CYP2C19, CYP2D6 and CYP3A4/3A5 were α-naphthoflavone (1 μM), sulfaphenazole (10 μM), troglitazone (10 μM), quinidine (1 μM), and ketoconazole (1 μM), respectively. β-eudesmol (10 μM) was pre-incubated with 0.2 mg/mL of HLM and selective inhibitors in 100 mM KPB (pH 7.4) at 37°C for 5 min. The reaction was initiated by adding 1 mM NADPH and further incubated for 15 min. After terminating the reaction, the sample was prepared, and β-eudesmol concentration was determined. The corresponding positive control was prepared without the addition of selective inhibitors, and the negative control was incubated without selective inhibitors and NADPH. The remaining amount of β-eudesmol in the test and positive systems was calculated using a negative system as a control, according to the previously described equation.

2.7 | Analysis of CYP enzyme kinetics

The enzyme kinetic parameters of β-eudesmol metabolism in the microsomal system were determined using the substrate depletion method. The reaction mixture of 200 μL, containing β-eudesmol (7.5–150 μM) and HLM (0.2 mg/mL) in 100 mM KPB (pH 7.4) was pre-incubation at 37°C for 5 min. Then, the reaction was initiated by adding 1 mM NADPH and further incubated at 37°C for 0–40 min. After the specified time point, the reactions were terminated, and the sample was prepared to determine β-eudesmol concentration. A control without the addition of NADPH was prepared simultaneously. The remaining amount of β-eudesmol was calculated.

The natural logarithm of the remaining amount of β-eudesmol (%) versus time was plotted to determine the first-order depletion rate constant (K_{dep}) for each concentration. The Michaelis–Menten constant, K_m, was estimated by plotting the K_{dep} versus substrate concentration. Maximum velocity (V_{max}) was calculated from $CL_{int} \times K_m$, where CL_{int} was determined from the

single-concentration substrate depletion of the metabolic intrinsic clearance investigation.

2.8 | Data analysis

The statistical analyses were performed utilizing IBM SPSS software, version 25 (IBM, NY, USA). Non-normally distributed quantitative variables are presented as median (95% CI). The Mann–Whitney U test was applied to compare the differences between the two quantitative groups. The statistical significance level of all tests was set at $\alpha = 0.05$.

3 | RESULTS

3.1 | HPLC analysis method validation

The analytical method for the determination of β-eudesmol was shown to be sensitive and specific (Figure S1). All calibration curves (peak height ratio of β-eudesmol to 1,8-dihydroxyantraquinone, internal standard) were linear with a correlation coefficient (r^2) greater than 0.995 (refer to Figure S2 as an example). The limit of quantitation (LOQ) of β-eudesmol at a signal-to-noise ratio ≥ 10 was 5 μM. The intraday and interday precision (%RSD: relative standard deviation) and accuracy (%Bias) of the analytical method ranged from 2.31% to 11.66% and − 3.22% to 17.91%, respectively (Table S2).

3.2 | Optimization of β-eudesmol and microsomal protein concentration, and incubation time

Following the incubation of β-eudesmol (10–30 μM) with HLM (0.2–0.5 mg/mL) for 10–40 min, the amount of β-eudesmol was decreased linearly with HLM concentration and incubation time (Figure 1). The remaining amounts of β-eudesmol was reduced to 50% of the initial concentrations after 20 min of incubation with β-eudesmol 10 μM and 20 μM. The amount was dropped to 50% after 40 min at the initial concentration of 30 μM. The percentage remaining amounts of β-eudesmol over time at various concentrations of microsomal protein and substrate are presented in Table S3. To avoid the use of higher substrate concentration in relation to the predicted K_m and to prevent the high turnover rate of β-eudesmol, the concentrations of HLM and β-eudesmol selected for further experiments were 0.2 mg/mL and 10 μM, respectively. The incubation period of 15 min was selected to ensure that the remaining amount of β-eudesmol was detectable by the validated analytical method.

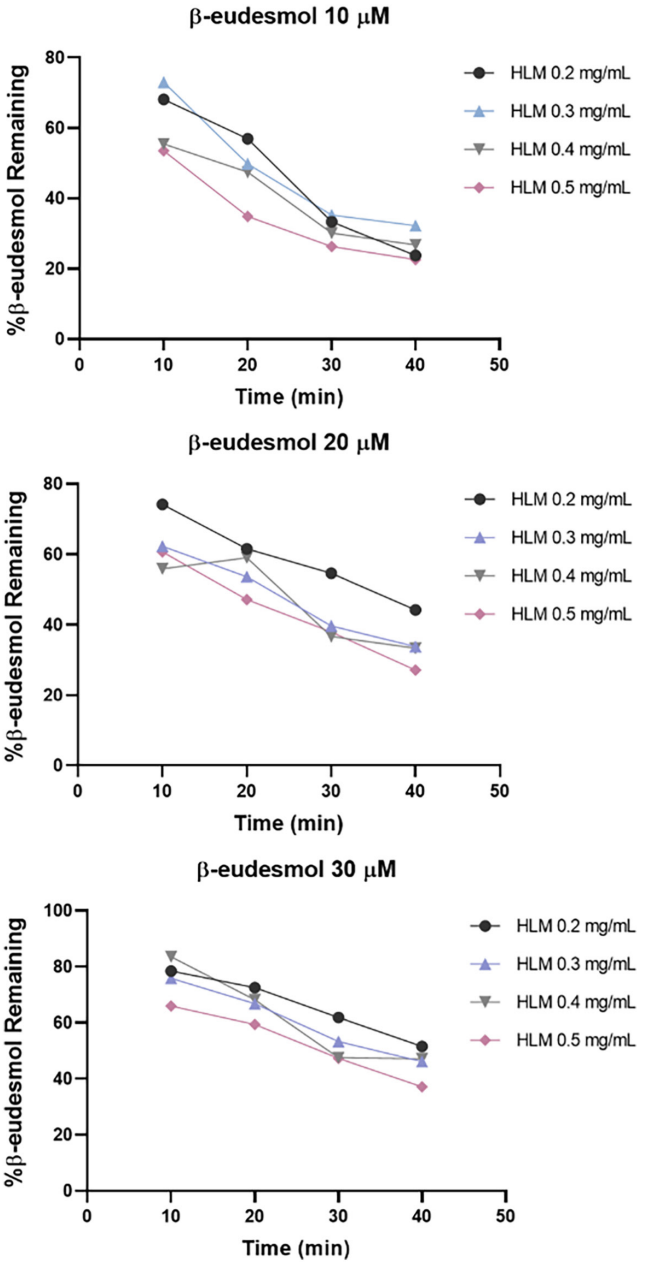

FIGURE 1 The depletion of β-eudesmol over time at various concentrations of microsomal proteins and substrate. β-eudesmol at the concentration range of 10–30 μM was incubated with HLM (0.2–0.5 mg/mL) and NADPH (1 mM) for 10–40 min.

3.3 | Metabolic stability and intrinsic clearance of β-eudesmol

After incubation of β-eudesmol (10 μM) with HLM (0.2 mg/mL) in the presence of the cofactor NADPH for 0–30 min, $t_{1/2}$ and the CL_{int} were 17.09 min and 0.20 mL/min·mg protein, respectively. The plot between the depletion of β-eudesmol versus incubation time and the percentage remaining amounts of β-eudesmol are presented in Figure 2 and Table S4, respectively.

3.4 | Assay with recombinant human CYP isoforms

rCYP1A2, rCYP2C9, rCYP2C19, rCYP2D6 and rCYP3A4 were selected for identification of the involvement of CYPs in the metabolism of β-eudesmol. Figure 3 and Table S5 depict the percentage

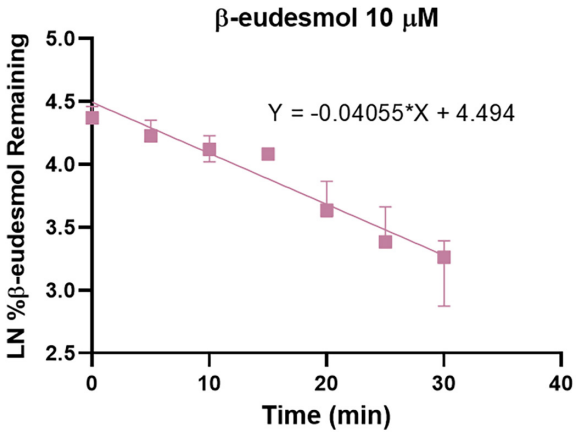

FIGURE 2 The depletion of β-eudesmol over time. The depletion of β-eudesmol was analyzed by incubating β-eudesmol (10 μM) with HLM (0.2 mg/mL) in the presence of NADPH (1 mM). The samples were collected at predetermined time points, and the concentration of β-eudesmol was then measured. Data are presented as the median (range) of three independent experiments.

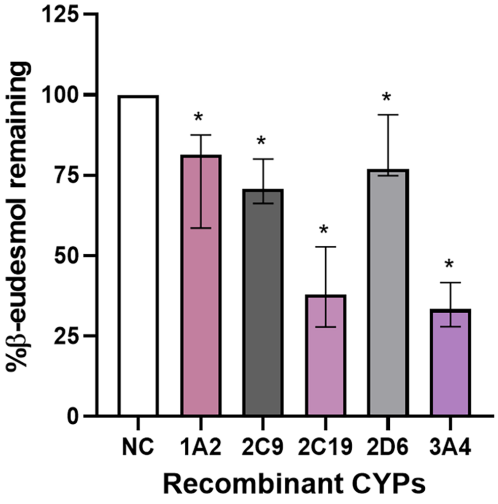

FIGURE 3 The remaining amounts of β-eudesmol following incubation with human recombinant CYPs (rCYP1A2, rCYP2C9, rCYP2C19, rCYP2D6 and rCYP3A4). β-Eudesmol (10 μM) was incubated with rCYPs and NADPH (1 mM) for 15 min. The Mann–Whitney U test was applied to compare the differences between each two groups. Data are presented as median (95% CI) from two independent experiments, triplicate each. *$p = .002$ compared to the negative control (NC).

of the remaining amounts of β-eudesmol after 15 min of incubation with each rCYP isoform. The remaining amount of β-eudesmol in the negative control without NADPH was considered 100%. A significant reduction in the amount of β-eudesmol was observed with all rCYP isoforms ($p = .002$). The most significant reduction was found with rCYP2C19 and rCYP3A4 [median (95% CI) of the remaining amounts of β-eudesmol: 37.86 (27.86–52.71)% and 33.32 (27.94–41.58)%, respectively]. For other rCYP isoforms, however, the disappearance of β-eudesmol varied from 20% to 25%.

3.5 | Assays with chemical inhibitors of CYPs

The contribution of CYPs in the metabolism of β-eudesmol was further confirmed by incubating β-eudesmol with a selective inhibitor for each CYP isoform in the NADPH-containing HLM system. The remaining amount of β-eudesmol was considered 100% for the negative control without a selective chemical inhibitor and NADPH. The incubation system in the presence of NADPH but without a selective inhibitor served as the positive control. Figure 4 and Table S6 show the remaining amounts of β-eudesmol after 15 min of incubation with selective chemical inhibitors. Compared with negative control, the remaining amount of β-eudesmol was significantly lower in both the positive control and test systems ($p = .002$ for CYP2C9, CYP2C19, CYP2D6; $p = .003$ for positive control, $p = .004$ for CYP1A2; and $p = .04$ for CYP3A4). Compared with the positive control, the significantly higher level of remaining amounts of β-eudesmol was observed only with CYP2C19 and CYP3A4 systems ($p = .028$) [median (95% CI): 51.29 (45.98–74.63)%, 72.52 (60.00–82.35)% and 74.11 (58.53–101.05)% for positive control, CYP2C19 and CYP3A4, respectively].

3.6 | Analysis of CYP enzyme kinetics

The kinetics of CYP-mediated metabolism of β-eudesmol was investigated by incubating the compound in an NADPH-containing HLM system. The concentrations of β-eudesmol used were 7.5, 10, 20, 30, 40, 60, 100, and 150 μM. The natural logarithm of the remaining amount of β-eudesmol (%) over time for each concentration which provides K_{dep} values, is shown in Figure 5 and Table S7. Based on the plot between K_{dep} and substrate concentration (Figure 6), the K_m and V_{max} were 16.76 μM and 3.35 nmol/min·mg protein, respectively.

4 | DISCUSSION

In the past decades, there has been a substantial increase in interest and exploration of herbal products as a complementary and alternative medicine for the prevention and treatment of various diseases.[26] In addition, concurrent use of multiple medications, including herbal medicine, has been increasing.[27,28] Although herbal medicines are widely used and are considered safe due to the long history of their traditional uses, their complex chemical composition raises concerns regarding potential interactions with other traditional products or prescribed medications.

The CYP modulatory activities of the AL and its major active compounds, atractylodin, and β-eudesmol, have been investigated both in vitro and in vivo.[13–15] Nevertheless, there is currently no available study that identifies the specific CYP enzyme(s) responsible for the metabolism of AL or its major constituents. This knowledge gap motivated our study to investigate the metabolizing enzyme(s) involved in AL metabolism using β-eudesmol as the marker compound due to its relatively high quantity (6%) and stability at body temperature (Table S1). Since certain amount of β-eudesmol was lost

during incubation due to the effect of temperature, we employed an incubation system that excluded NADPH as a control for each specific time point. Despite atractylodin being the most abundant in AL rhizome (14%), its instability at incubation temperature (37°C) precluded its use as the marker compound for this investigation.

This study selected the concentration of β-eudesmol based on the reaction phenotyping investigation protocol. Although the recommended initial substrate concentration is typically lower than K_m (≤1 μM),[29] β-eudesmol at a higher concentration of 10 μM was selected to improve the sensitivity of the HPLC analysis. The five major human CYPs, namely, rCYP1A2, rCYP2C9, rCYP2C19, rCYP2D6, and rCYP3A4, were selected for the phenotyping investigation.

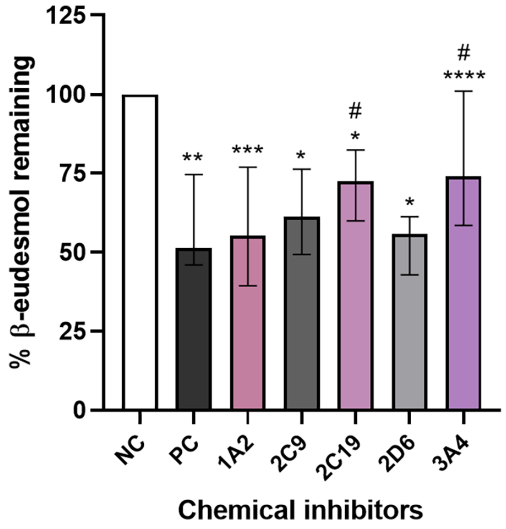

FIGURE 4 The remaining amounts of β-eudesmol following incubation with selective chemical inhibitors of CYP1A2, CYP2C9, CYP2C19, CYP2D6, and CYP3A4. β-eudesmol (10 μM) was incubated with HLM (0.2 mg/mL) and NADPH (1 mM) in the presence or absence of selective inhibitors for 15 min. The Mann–Whitney U test was applied to compare the differences between each two groups. Data are presented as median (95% CI) from two experiments triplicate each. *p = .002, **p = .003, ***p = .004, ****p = .04 compared to the negative control (NC) and $^{\#}p$ = .028 compared to the positive control (PC).

During the incubation of β-eudesmol with each rCYP, a significant disappearance profile of β-eudesmol was observed, suggesting possible contributions of these five CYP enzymes to the biotransformation of β-eudesmol. However, upon using selective chemical inhibitors for each CYP in the HLM system, a significant higher level in the remaining β-eudesmol was only evident in the presence of CYP2C19 and CYP3A4 inhibitors compared with the positive control (the incubation system in the presence of NADPH but without a selective inhibitor). This specific pattern of disappearance strongly indicates that CYP2C19 and CYP3A4 substantially contribute to the metabolism of β-eudesmol. Our earlier research showed that β-eudesmol acts as an inhibitor of rCYP2C19 and rCYP3A4.[15] This may suggest that β-eudesmol might have a dual role, functioning both as an inhibitor and a substrate for these CYP enzymes. In another previous study involving ligand-binding spectroscopy of rCYPs prepared using *Escherichia coli* membrane, considerable binding of β-eudesmol to CYP1A2 and CYP3A4, but not CYP2C9, CYP2C19, and CYP2D6 were reported.[30] The discrepancy between the current and previous studies might be due to the different techniques applied in the experiments. Furthermore, binding affinity could be affected by several factors, including conformation of rCYP, substrate concentration, and the ability to escape rCYP of the ligand, β-eudesmol.[31]

The final experiment for the reaction phenotyping was the determination of CYP enzyme kinetics in the HLM system. Due to the unavailability of technical analysis to identify metabolite(s) of β-eudesmol, we utilized the substrate depletion method for enzyme kinetic analysis.[29] Based on the plot between depletion constant and substrate concentration, the K_m of 16.76 μM was higher than the concentration of β-eudesmol (10 μM) used in earlier experiments. This was due to a relatively low concentration of HLM used in the study, which provided a moderate turnover rate of β-eudesmol. The estimated V_{max} was an approximate value due to the high initial concentration of β-eudesmol used for CL_{int} and K_m determination. The K_m and V_{max} indicate the enzyme affinity for the substrate and its catalytic activity, respectively, while CL_{int} indicates the efficiency of an enzyme-catalyzed reaction. Although specific cut-off values for both parameters are not available, the estimated K_m value is relatively high, suggesting the lower affinity of β-eudesmol to microsomal CYP

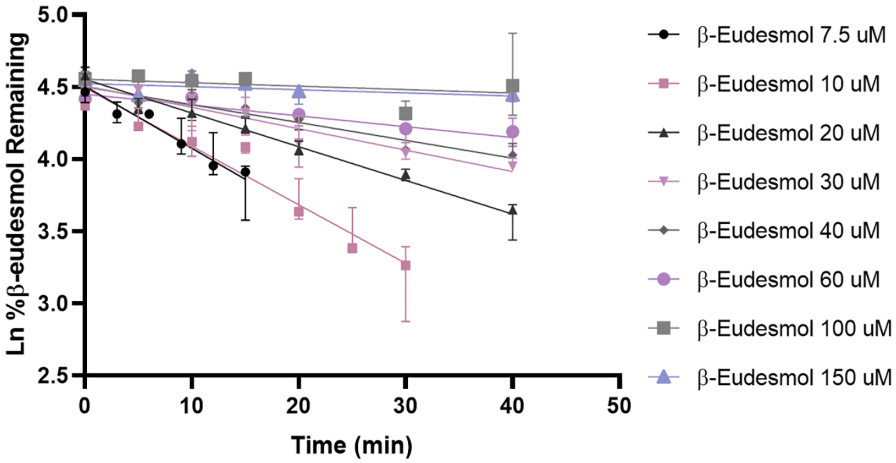

FIGURE 5 The depletion of β-eudesmol at various concentrations. β-eudesmol at the concentration range of 7.5–150 μM were incubated with HLM (0.2 mg/mL) in the presence of NADPH. The samples were collected at specified time points. Data are presented as the median (range) of three independent experiments.

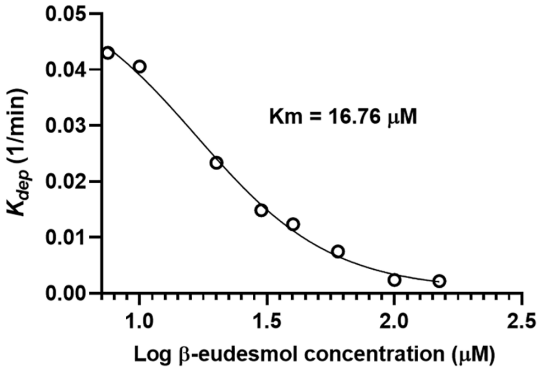

FIGURE 6 The plot of in vitro depletion rate constants, K_{dep}, versus β-eudesmol concentrations.

enzymes compared with other compounds reported in previous studies.[32,33] Additionally, the estimated V_{max} and CL_{int} from the current study were high, which may suggest slight elevation of catalytic activity and the efficiency of enzyme-catalyzed reactions. The variation in the estimation values is likely attributed to the use of an analytical method with low sensitivity. To achieve accurate estimation therefore, high concentrations of β-eudesmol were used in the experiment. Furthermore, as recommended, the substrate concentration used for CL_{int} determination should be ≤1 μM, and the K_m should be calculated from 50% of the theoretical maximum rate at a very low substrate concentration. Therefore, to obtain precise values for K_m, V_{max}, and CL_{int}, it is imperative to employ a high-sensitivity analytical method for the determination of β-eudesmol, which would enhance analytical efficiency, particularly at lower concentrations of β-eudesmol.

Several anticancer agents used for CCA treatment are substrates of CYPs, including docetaxel (CYP3A4),[20] irinotecan (CYP2B6 and CYP3A4),[21,22] paclitaxel (CYP2C8, CYP2C9, and CYP3A4),[21,23] and erlotinib (CYP3A4).[21,24] Some anticancer drugs are also the inhibitors of CYPs, such as capecitabine (CYP2C9), 5-FU (CYP2C9) and sorafenib (CYP2B6, 2C8, 2C9).[21] Moreover, several drugs used for supportive care during cancer treatment and concurrent diseases or symptoms, particularly venous thromboembolism (VTE), were reported to modulate CYP3A4 activity. These included antiemetic drugs (ondansetron and aprepitant) and antithrombotic drugs (rivaroxaban, apixaban, and edoxaban), which are substrates of CYP3A4, and antifungal drugs (fluconazole and itraconazole) which are inhibitors of CYP3A4.[34,35] Given that AL has been developed for clinical use as an adjunctive therapy for CCA, it is likely to be co-administered with first-line chemotherapeutic drugs. This co-administration could potentially lead to interactions with these medications due to β-eudesmol acting as a substrate and inhibitor for CYP2C19 and CYP3A4 enzymes.

Our study highlights potential information for protecting against herb–drug interactions. However, certain limitations exist, including the absence of a highly sensitive analytical method for β-eudesmol determination at low concentrations and the unavailability of an analytical approach for identifying β-eudesmol metabolites. To deepen our understanding of β-eudesmol metabolism and its associated pathway, the sensitive and specific analytical method for metabolite identification should be developed. Furthermore, exploring β-eudesmol metabolism involving non-CYP enzymes could yield valuable insights and assist in reducing the risk of herb-drug interactions when combining AL with standard chemotherapy in CCA patients.

5 | CONCLUSION

The CYP enzymes, particularly CYP2C19 and CYP3A4 isoforms, play a significant role in β-eudesmol metabolism. As a component of AL, β-eudesmol as a substrate and inhibitor of CYP2C19 and CYP3A4, has a high potential for drug–drug interactions when AL is co-administered with other herbs or conventional medicines.

AUTHOR CONTRIBUTIONS

Nadda Muhamad: Participated in research design, conducted experiments, performed data analysis, and wrote, reviewed, and edited the manuscript. Kesara Na-Bangchang: Participated in research design, contributed reagents and analytic tools, and wrote, reviewed, and edited the manuscript.

ACKNOWLEDGMENTS

None.

FUNDING INFORMATION

This study was supported by Thammasat University Research Fund, Contract No. TUFT-FF 48/2565 and Thailand Science Research and Innovation Fundamental Fund. Nadda Muhamad was supported by Thailand Research Fund under the Royal Golden Jubilee Ph.D. Program (grant number PHD/0095/2561). Kesara Na-Bangchang was supported by Center of Excellence in Pharmacology and Molecular Biology of Malaria and Cholangiocarcinoma.

CONFLICT OF INTEREST STATEMENT

The authors declare no conflicts of interest.

DATA AVAILABILITY STATEMENT

The data that support the findings of this study are available from the corresponding author, Kesara Na-Bangchang, upon reasonable request.

ETHICS STATEMENT

This research does not involve human or animal subjects, and ethical permission is not required.

ORCID

Nadda Muhamad https://orcid.org/0000-0002-0954-9687
Kesara Na-Bangchang https://orcid.org/0000-0001-6389-0897

REFERENCES

1. Koonrungsesomboon N, Na-Bangchang K, Karbwang J. Therapeutic potential and pharmacological activities of Atractylodes lancea (Thunb.) DC. *Asian Pac J Trop Med*. 2014;7:421-428.

2. Kotawong K, Chaijaroenkul W, Muhamad P, Na-Bangchang K. Cytotoxic activities and effects of atractylodin and β-eudesmol on the cell cycle arrest and apoptosis on cholangiocarcinoma cell line. *J Pharmacol Sci*. 2018;136:51-56.
3. Plengsuriyakarn T, Matsuda N, Karbwang J, Viyanant V, Hirayama K, Na-Bangchang K. Anticancer activity of Atractylodes lancea (Thunb.) DC in a hamster model and application of PET-CT for early detection and monitoring progression of cholangiocarcinoma. *Asian Pac J Cancer Prev*. 2015b;16:6279-6284.
4. Plengsuriyakarn T, Viyanant V, Eursitthichai V, et al. Anticancer activities against cholangiocarcinoma, toxicity and pharmacological activities of Thai medicinal plants in animal models. *BMC Complement Altern Med*. 2012a;12:23.
5. Plengsuriyakarn T, Viyanant V, Thitapakorn V, Itharat A, Na-bangchang K. In vitro investigations on the potential roles of Thai medicinal plants in treatment of cholangiocarcinoma. *Int Res Pharm Pharmacol*. 2012b;2:52-63.
6. Martviset P, Chaijaroenkul W, Muhamad P, Na-Bangchang K. Bioactive constituents isolated from Atractylodes lancea (Thunb.) DC. rhizome exhibit synergistic effect against cholangiocarcinoma cell. *J Exp Pharmacol*. 2018;10:59-64.
7. Plengsuriyakarn T, Karbwang J, Na-Bangchang K. Anticancer activity using positron emission tomography-computed tomography and pharmacokinetics of β-eudesmol in human cholangiocarcinoma xenografted nude mouse model. *Clin Exp Pharmacol Physiol*. 2015a;42:293-304.
8. Na-Bangchang K, Plengsuriyakarn T, Karbwang J. Research and development of Atractylodes lancea (Thunb) DC. as a promising candidate for cholangiocarcinoma chemotherapeutics. *Evid Based Complement Alternat Med*. 2017;2017:5929234.
9. Na-Bangchang K, Kulma I, Plengsuriyakarn T, et al. Phase I clinical trial to evaluate the safety and pharmacokinetics of capsule formulation of the standardized extract of Atractylodes lancea. *J Tradit Complement Med*. 2021;11:343-355.
10. Goodman LS, Gilman A, Brunton LL, Chabner B, BrC K. *Goodman & Gilman's the Pharmacological Basis of Therapeutics*. McGraw-Hill; 2011.
11. Evans WE, Relling MV. Pharmacogenomics: translating functional genomics into rational therapeutics. 1999;286:487-491.
12. Martinez MN, Antonovic L, Court M, et al. Challenges in exploring the cytochrome P450 system as a source of variation in canine drug pharmacokinetics. *Drug Metab Rev*. 2013;45:218-230.
13. Sumsakul W, Mahavorasirikul W, Na-Bangchang K. Inhibitory activities of Thai medicinal plants with promising activities against malaria and cholangiocarcinoma on human cytochrome P450. *Phytother Res*. 2015;29:1926-1933.
14. Muhamad N, Plengsuriyakarn T, Na-Bangchang K. Atractylodes lancea for cholangiocarcinoma: modulatory effects on CYP1A2 and CYP3A1 and pharmacokinetics in rats and biodistribution in mice. *PloS One*. 2022;17:e0277614.
15. Thiengsusuk A, Plengsuriyakarn T, Na-Bangchang K. Modulatory effects of atractylodin and β-eudesmol on human cytochrome p450 enzymes: potential drug-drug interactions. *Molecules*. 2023;28:3140.
16. Zientek MA, Youdim K. Reaction phenotyping: advances in the experimental strategies used to characterize the contribution of drug-metabolizing enzymes. *Drug Metab Dispos*. 2015;43:163-181.
17. Zhou SF. Polymorphism of human cytochrome P450 2D6 and its clinical significance: part I. *Clin Pharmacokinet*. 2009;48:689-723.
18. Wang B, Wang J, Huang SQ, Su HH, Zhou SF. Genetic polymorphism of the human cytochrome P450 2C9 gene and its clinical significance. *Curr Drug Metab*. 2009;10:781-834.
19. Pang YS, Wong LP, Lee TC, Mustafa AM, Mohamed Z, Lang CC. Genetic polymorphism of cytochrome P450 2C19 in healthy Malaysian subjects. *Br J Clin Pharmacol*. 2004;58:332-335.
20. Kenmotsu H, Tanigawara Y. Pharmacokinetics, dynamics and toxicity of docetaxel: why the Japanese dose differs from the Western dose. *Cancer Sci*. 2015;106:497-504.
21. Amanda HC. *Drug Information Handbook with International Trade Names Index*. 24th ed. Hudson; 2015.
22. Santos A, Zanetta S, Cresteil T, et al. Metabolism of irinotecan (CPT-11) by CYP3A4 and CYP3A5 in humans. *Clin Cancer Res*. 2000;6:2012-2020.
23. Spratlin J, Sawyer MB. Pharmacogenetics of paclitaxel metabolism. *Crit Rev Oncol Hematol*. 2007;61:222-229.
24. Smith NF, Baker SD, Gonzalez FJ, Harris JW, Figg WD, Sparreboom A. Modulation of erlotinib pharmacokinetics in mice by a novel cytochrome P450 3A4 inhibitor, BAS 100. *Br J Cancer*. 2008;98:1630-1632.
25. ICH. ICH guideline Q2(R2) on validation of analytical procedures, in. 2022 https://database.ich.org/sites/default/files/ICH_Q2-R2_Document_Step2_Guideline_2022_0324.pdf
26. Hermann R, Von Richter O. Clinical evidence of herbal drugs as perpetrators of pharmacokinetic drug interactions. *Planta Med*. 2012;78:1458-1477.
27. Asiimwe JB, Nagendrappa PB, Atukunda EC, et al. Prevalence of the use of herbal medicines among patients with cancer: a systematic review and meta-analysis. *Evid Based Complement Alternat Med*. 2021;2021:9963038.
28. Irmak Z, Tanrıverdi Ö, Ödemiş H, Uysal DD. Use of complementary and alternative medicine and quality of life of cancer patients who received chemotherapy in Turkey. *Complementary Ther Med*. 2019;44:143-150.
29. Sensenhauser C. In vitro CYP/FMO reaction phenotyping. In: Caldwell GW, Yan Z, eds. *Optimization in Drug Discovery: In Vitro Methods*. Humana Press; 2014:137-169.
30. Krenc D, Na-Bangchang K. Spectroscopic observations of β-eudesmol binding to human cytochrome P450 isoforms 3A4 and 1A2, but not to isoforms 2C9, 2C19, and 2D6. *Xenobiotica*. 2022;52:199-208.
31. Conner KP, Woods CM, Atkins WM. Interactions of cytochrome P450s with their ligands. *Arch Biochem Biophys*. 2011;507:56-65.
32. Dai ZR, Ning J, Sun GB, et al. Cytochrome P450 3A enzymes are key contributors for hepatic metabolism of bufotalin, a natural constitute in chinese medicine Chansu. *Front Pharmacol*. 2019;10:52.
33. Zhuang XM, Chen L, Tan Y, et al. Identification of human cytochrome P450 and UGT enzymes involved in the metabolism of ferulic acid, a major bioactive component in traditional Chinese medicines. *Chin J Nat Med*. 2017;15:695-702.
34. Lenoir C, Terrier J, Gloor Y, et al. Impact of the genotype and phenotype of cyp3a and p-gp on the apixaban and rivaroxaban exposure in a real-world setting. *J Pers Med*. 2022;12:1-21.
35. Tsoukalas N, Brito-Dellan N, Font C, et al. Complexity and clinical significance of drug-drug interactions (DDIs) in oncology: challenging issues in the care of patients regarding cancer-associated thrombosis (CAT). *Support Care Cancer*. 2022;30:8559-8573.

SUPPORTING INFORMATION

Additional supporting information can be found online in the Supporting Information section at the end of this article.

How to cite this article: Muhamad N, Na-Bangchang K. The roles of CYP2C19 and CYP3A4 in the in vitro metabolism of β-eudesmol in human liver: Reaction phenotyping and enzyme kinetics. *Pharmacol Res Perspect*. 2023;11:e01149. doi:10.1002/prp2.1149